ACADEMIC PRESS

Available online at www.sciencedirect.com

SCIENCE DIRECT®

DEVELOPMENTAL BIOLOGY

Developmental Biology 264 (2003) 275–288

www.elsevier.com/locate/ydbio

Pericyte production of cell-associated VEGF is differentiation-dependent and is associated with endothelial survival

D.C. Darland,[a] L.J. Massingham,[a] S.R. Smith,[b] E. Piek,[c,1] M. Saint-Geniez,[a] and P.A. D'Amore[a,b,d,*]

[a] *Schepens Eye Research Institute and the Department of Ophthalmology, Harvard Medical School, Boston, MA 02114, USA*
[b] *Children's Hospital, Harvard Medical School, Boston, MA 02115, USA*
[c] *National Cancer Institute, National Institutes of Health, Bethesda, MD 20892, USA*
[d] *Department of Pathology, Harvard Medical School, Boston, MA 02115, USA*

Received for publication 28 March 2003, revised 28 July 2003, accepted 15 August 2003

Abstract

Pericytes have been suggested to play a role in regulation of vessel stability; one mechanism for this stabilization may be via pericyte-derived vascular endothelial growth factor (VEGF). To test the hypothesis that differentiation of mesenchymal cells to pericytes/smooth muscle cells (SMC) is accompanied by VEGF expression, we used endothelial cell (EC) and mesenchymal cell cocultures to model cell–cell interactions that occur during vessel development. Coculture of EC and 10T1/2 cells, multipotent mesenchymal cells, led to induction of VEGF expression by 10T1/2 cells. Increased VEGF expression was dependent on contact between EC-10T1/2 and was mediated by transforming growth factorβ (TGFβ). A majority of VEGF produced in coculture was cell- and/or matrix-associated. Treatment of cells with high salt, protamine, heparin, or suramin released significant VEGF, suggesting that heparan sulfate proteoglycan might be sequestering some of the VEGF. Inhibition of VEGF in cocultures led to a 75% increase in EC apoptosis, indicating that EC survival in cocultures is dependent on 10T1/2-derived VEGF. VEGF gene expression in developing retinal vasculature was observed in pericytes contacting newly formed microvessels. Our observations indicate that differentiated pericytes produce VEGF that may act in a juxtacrine/paracrine manner as a survival and/or stabilizing factor for EC in microvessels.

Introduction

Vascular development is a complex process that begins with the formation of a primary capillary plexus via angiogenesis or vasculogenesis and ends when the primitive vessels have been remodeled into quiescent, differentiated vessels. Differentiated, "mature" vessels are characterized histologically by associated pericytes/smooth muscle cells (SMC) and a mature basement membrane. The cellular and molecular regulation of vascular remodeling is the object of much scrutiny, and results from in vitro and in vivo systems have provided some insight. The angiogenesis factor, vascular endothelial growth factor (VEGF), and its receptors have been shown to be required for vessel assembly both in vivo (Carmeliet et al., 1996; Ferrara et al., 1996) and in vitro (Fong et al., 1999). Platelet-derived growth factor BB (PDGF-BB), produced by immature endothelial cells (EC), stimulates mesenchymal cell proliferation and migration toward the EC in vitro (Hirschi et al., 1998) and the forming vessel in vivo (Hellström et al., 1999; Lindahl et al., 1997). Results from coculture models suggest that transforming growth factor β1 (TGFβ1) that is activated upon contact between EC and mesenchymal cells inhibits EC proliferation and migration (Antonelli-Orlidge et al., 1989; Sato et al., 1990) and induces pericyte/SMC differentiation (Hirschi et al., 1998; Darland and D'Amore, 2001). Whereas a number of the molecular players that mediate vessel assembly have been identified, less is known about the cellular and molecular control of vessel remodeling and stabilization.

* Corresponding author. Fax: +1-617-912-0128.
E-mail address: pdamore@vision.eri.harvard.edu (P.A. D'Amore).
[1] Current address: Department of Cell Biology & Applied Biology Catholic University Nijmegan Toernooiveld 1, 6525 ED Nijmeagen, The Netherlands.

0012-1606/$ – see front matter © 2003 Elsevier Inc. All rights reserved.
doi:10.1016/S0012-1606(03)00492-5

Pericytes have been suggested to play a role in vessel maturation, and there is increasing evidence to indicate that pericytes influence vessel stability. For example, there appears to be a correlation between pericyte number and vessel stability; brain and retina, which have the highest density of pericytes, have the lowest turnover rate (Denekamp, 1982; Engerman et al., 1967). Pericytes have been shown to suppress EC proliferation (Antonelli-Orlidge et al., 1989; Hirschi et al., 1999) and migration (Sato and Rifkin, 1989) in vitro, and the loss of pericytes in diabetic retinopathy precedes retinal EC proliferation (Kuwabara and Cogan, 1963; Crocker et al., 1970). In an experimental model, retinal vessels lacking pericytes were prone to regression in vivo (Benjamin et al., 1998). In addition, the absence of pericytes in the brain microvasculature of mice deficient in the PDGFβ receptor or the PDGF-BB ligand has been correlated with EC hyperplasia (Hellström et al., 2001), lending further credence to a role for pericytes in suppression of EC proliferation and in stabilization of vessels.

Evidence from a variety of systems suggests that immature/developing vessels are dependent on tissue-derived VEGF. For instance, experimentally induced vessel regression in the developing murine retina can be blocked by administration of exogenous VEGF (Alon et al., 1995). Similarly, using a human prostate tumor cell model of inducible VEGF expression, it was demonstrated that VEGF loss resulted in selective EC death by apoptosis in vessels that lacked pericytes (Benjamin et al., 1999). Thus, we hypothesized that pericyte stabilization of vessels might be mediated by pericyte production of VEGF. In order to investigate whether pericyte-derived VEGF might be involved in vessel stabilization, we have used a coculture system to model the heterotypic cell–cell interactions that occur between pericyte precursors and EC and to examine production of VEGF. In the current study, we test the hypothesis that the differentiation of mesenchymal cells to pericytes/SMC is correlated with the induction of VEGF expression, and that this VEGF is associated with EC survival and vessel stability. Our findings of VEGF production by differentiating pericytes in two- and three-dimensional coculture systems as well as in vivo point to a role for pericyte-derived VEGF in vessel stabilization.

Materials and methods

Cell culture

C3H/10T1/2 mouse mesenchymal cells (10T1/2; ATCC, Rockville, MD) and bovine aortic EC were grown in Dulbecco's modified Eagle's medium (DMEM, JRH Biosciences, Lenexa, KS) supplemented with 10% fetal calf serum (FCS, Hyclone Laboratories, Logan, UT), 233.6 μg/ml glutamine, 80 units/ml penicillin, 80 μg/ml streptomycin (GPS; Irvine Scientific, Santa Ana, CA), and 25 mM glucose (Sigma Chemical Company, St. Louis, MO). The homogeneity of the EC was confirmed by DiI-acetylated LDL uptake (Biomedical Technologies, Stoughton, MA). The cells were used under passage 20 and were maintained at confluence for 3 days prior to use. Mouse embryo fibroblasts (MEF) from wild type and *smad 3* null mice were isolated as described (Piek et al., 2001) and were grown in DMEM/10% FCS/GPS and used between passages 6 and 8. Cell counts were determined by using a Z1 Particle Counter (Coulter Corporation; Miami, FL).

Cocultures

Direct coculture

EC and 10T1/2 cells were plated alone or as cocultures (1.5×10^5 cells/35 mm^2 dish or 2.5×10^5 cells/well in a 6-well tissue culture dish) in DMEM/10% FCS/GPS. After 90 min, the medium was removed and replaced with serum-free DMEM/GPS. Recombinant human TGFβ1 (R&D Systems, Minneapolis, MN) was added where indicated at 1 ng/ml (time course) or at 3 ng/ml (direct and Transwell culture). These concentrations were selected on the basis of dose response curves for stimulating 10T1/2 differentiation to pericytes.

Transwell coculture

EC and 10T1/2 cells were cultured alone or as cocultures (1.5×10^5 of each cell type) in 6-well Transwells (Corning Inc, Corning, NY) for 72 h with or without TFGβ1. The EC were plated in DMEM/10%CS/GPS at 37°C on the underside of the Transwells. After 90 min, the Transwells were reinserted into the 6-well plate and 10T1/2 were plated in the upper chamber of the Transwell. After 90 min, the cells were washed once with serum-free medium, and 2 ml of serum-free medium were added to each well with or without 3 ng/ml TGFβ1.

VEGF ELISA

Conditioned medium (CM) was removed from the Transwells and 0.1% Tween 20 and protease inhibitors (2 μg/ml aprotinin, 5 μg/ml leupeptin, 10 μg/ml phenylmethyl sulfonyl fluoride, and 10 mM sodium fluoride; Sigma) were added. The cells were gently washed with PBS and the cell-associated material was collected into 30 μl of lysis buffer containing 20 mM Tris (pH 8.0), 150 mM NaCl, 1 mM dithiothreitol, 1% deoxycholic acid, 0.5% sodium dodecylsulfate, 1% Nonidet P-40, and protease inhibitors (as above). A known concentration of total protein (5–10 μg) based on a D_c protein assay (BioRad, Hercules, CA) was assayed for each sample. CM and cell-associated material were stored at −80°C prior to analysis and were used to determine levels of VEGF protein using a mouse VEGF ELISA kit that recognizes predominantly the VEGF120 and VEGF164 isoforms of VEGFA (R&D Systems). The intraassay and interassay variability had coefficients of vari-

Table 1
Proportional distribution of VEGF protein between cell-associated (CA) and conditioned medium (CM)

Condition	CA	CM
Direct culture		
10T1/2	53%	47%
10T1/2 + TGFβ1	42%	58%
10T1/2 + EC	71%	29%
Transwell culture		
10T1/2	52%	48%
10T1/2 + TGFβ1	52%	48%
10T1/2 + EC	74%	26%

ance of 8.2 and 8.4%, respectively, as determined by the manufacturer for the range of protein concentrations used in our assays. The minimum detectable concentration of VEGF is below 3 pg/ml. The A_{450} for each sample was determined relative to a VEGF dilution curve made from an internal standard. Values from independent experiments were compared with univariate analysis of variance (ANOVA) and Fischer's protected least significant difference (PLSD).

Western blot analysis

Cell-associated material (same material as was used for ELISA assays) was separated on 10% polyacrylamide gels and transferred to nitrocellulose filters as previously described (Darland and D'Amore, 2001). Filters were blocked in 5% nonfat powdered milk, 0.1% Tween 20 in PBS for 1 h at room temperature. A polyclonal antibody to NG2 proteoglycan (Chemicon International, Inc., Temecula, CA) was used at 1:1500. Filters were washed twice with alternating 0.2% Nonidet P-40 in PBS and 0.1% Tween 20 in PBS, 10 min each. The filters were incubated with the appropriate goat anti-rabbit coupled to horseradish peroxidase and diluted 1:5000 (Santa Cruz, Santa Cruz, CA). Washes were repeated as described and immunoreactive bands were visualized by using ECLPlus (Amersham) and detected on Hyper film (Amersham). The resulting images were scanned with Adobe Photoshop, and densitometric analysis was conducted by using NIH Image software (National Institutes of Health, Bethesda, MD; http://rsb.info.nih.gov/nih-image/). Protein concentration was determined with a D_c protein assay kit (BioRad) to ensure even loading of 8 μg of total protein. NG2 band density from three independent experiments was used to obtain the mean densitometric units, and statistical differences were determined by using ANOVA and Fischer's PLSD.

Three-dimensional (3D) cultures

The 3D cocultures were established by polymerizing 200 μl of Matrigel basement membrane extract (Fisher Scientific, Pittsburgh, PA) in 24-well tissue culture plates. 10T1/2 and EC were labeled with PKH67 (Sigma) and PKH26 (Sigma), respectively, according to the manufacturer's recommended protocol with modifications described previously (Darland and D'Amore, 2001). Cells were plated in normal growth medium at a density of 2.5×10^4 cells of each type per well on the Matrigel and were switched to serum-free medium after 1 h. The prelabeled cells in 3D cocultures were visualized by using a Dualband filter set for FITC/TRITC (51004v2 Excitation Filter, Micro Video Instruments, Avon, MA) on a Nikon inverted microscope. Cocultures were established in triplicate, and photos of four low-power fields of view were taken. Regions photographed in each well were chosen by using an ocular grid. Collectively, these fields covered approximately 18% of the total well surface area. In order to obtain a semiquantitative assessment of cord formation in the 3D cocultures, we compared cord length between control and treated cultures as previously described (Darland and D'Amore, 2001). In brief, the slides were scanned by using Adobe Photoshop, and each cord/structure was labeled for tracking and assessed for cord length (NIH Image). All data analysis was performed as a frequency distribution by using ANOVA and Fischer's PLSD. The initial assessment and quantification were conducted by an observer masked to treatment conditions. A subset of the analyses was repeated by an independent observer and similar results were obtained.

Identification of cell surface- and matrix-associated VEGF

Cocultures of EC and 10T1/2 were plated in normal growth medium at 1×10^5 cells of each type/well in 12-well plates and switched to serum-free medium after 90 min. After 3 days, the CM was collected and the cells were washed with 1 ml/well of Hank's balanced salt solution (HBSS, Sigma). The cells were incubated for 10 min at 37°C with 500 μl/well of HBSS, 2 M NaCl, 10 mg/ml protamine, 0.1% suramin (0.07 mM), or 100 mg/ml heparin (Sigma). All solutions were prepared in HBSS. The eluted material was collected and the remaining cell-associated material was obtained by scraping and shearing in a volume of 200 μl of lysis buffer (same as that used for Western assays). VEGF protein was quantified by ELISA assay as described above. The total VEGF in the sample was calculated as a sum of the eluted material and the cell-associated material and was used to determine the percentage of VEGF in the eluted material.

Detection of apoptotic cells

EC and 10T1/2 were plated in coculture on 4-well Permanox Lab-Tek Chamber slides (VWR, Bridgeport, NJ) at a total density of 3×10^4 cells/2cm^2 well. After 90 min, the plating medium was removed and replaced with serum-free medium containing either 25 μg/ml VEGF neutralizing an-

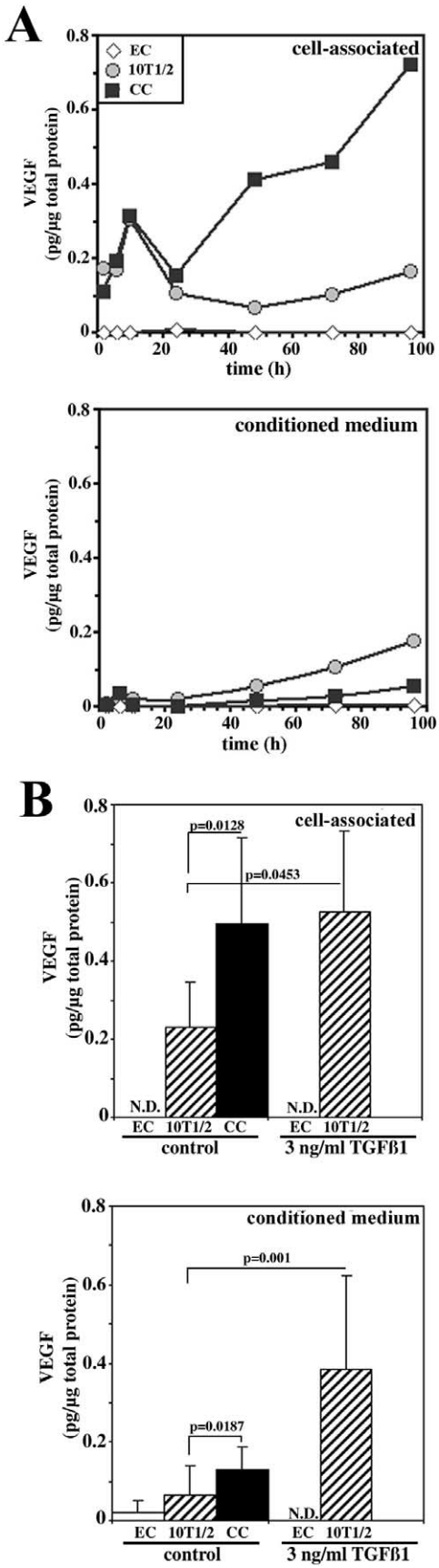

tibody or type-matched IgG as a negative control (Neomarkers, Fremont, CA). All conditions were plated in quadruplicate. The cultures were grown for 18 h, followed by fixation in 4% paraformaldehyde in PBS. Apoptotic cells were detected by using the DEADEnd assay kit (Promega, Madison, WI) according to the manufacturer's instructions. In order to identify 10T1/2 cells in the cocultures, the cells were immunostained for α-SMA using a 1:100 dilution of mouse anti-α-SMA (Dako) after DEADEnd processing. The secondary antibody, donkey anti-mouse IgG coupled to cy3 fluorochrome (Jackson Immunochemicals, West Grove, PA), was used at 1:250. Antibodies were diluted in a blocking solution consisting of 4% donkey serum/3% bovine serum albumin/0.1% Triton X-100 in PBS. All nuclei were identified by labeling for 15 min at RT with 500 ng/ml DAPI (Sigma). Sections were washed in PBS and permanently mounted with ProLong Antifade reagent (Molecular Probes, Eugene, OR). For quantification, UV fluorescence and bright field images were obtained with a CCD camera on a Nikon axiophot microscope. Two images were collected for each of four wells to determine the percentage of apoptotic nuclei and the cell number for a representative 1.2-mm^2 area. ANOVA and Fischer's PLSD were used to determine significance.

VEGF in developing retinal vasculature

Eyes were isolated from P7.5 or P9.5 mice heterozygous for the LacZ gene under control of the VEGF promoter (Miquerol et al., 1999). The mice were from a CD-1/129 hybrid background, and the LacZ gene with a nuclear localization signal was under an independent ribosome entry site inserted into the 3 prime untranslated region of the VEGF gene. Whole eyes were fixed for 24 h at 4°C in 4% paraformaldehyde and the retinas isolated. Retinas were permeabilized and blocked in 5% donkey serum, 5% goat serum, 0.1% saponin, 250 mM NaCl in PBS for 48 h at 4°C. The histochemical labeling of βgal activity was conducted overnight at 4°C using the in situ βgal kit (Stratagene, La Jolla, CA).

Trypsin digests were performed essentially as described

Fig. 1. Effect of EC-10T1/2 coculture and TGFβ on VEGF expression. (A) Solo and cocultures (CC) of 10T1/2 and EC were plated at 1.5×10^5 cells in 35-mm^2 dishes in medium containing 1% serum. The culture medium was changed at 72 h. Cell-associated material and CM from 10T1/2 in solo culture (gray circles), EC in solo culture (open diamonds), and 10T1/2 and EC in CC (black squares) were collected at time points indicated and analyzed for VEGF by ELISA. The experiment was repeated three times with similar results and a representative experiment is shown. (B) Solo and CC of 10T1/2 and EC were plated at 2.5×10^5 cells/well in 6-well tissue culture plates in complete medium. Ninety minutes after plating, the medium was removed and replaced with serum-free medium with or without 3 ng/ml TGFβ1. Cell-associated material and CM were collected at 3 days, and VEGF levels were determined by ELISA. The values shown are the mean and standard deviation of five independent experiments. N.D. is "not detectable."

(Mizutani et al., 1996). The eye cups were incubated for 4 h with 3% trypsin, 0.1 M Tris buffer, pH 7.8, and 0.2 M sodium fluoride. The tissue was washed repeatedly, and the remaining vascular web was removed by microdissection. For immunolabeling, the antibodies used included: mouse anti-βgal (1:400 Promega), rabbit anti-NG2 (1:200; Chemicon, Temecula, CA), rabbit anti-GFAP (1:400; Dako, Carpinteria, CA), and rat anti-PECAM (BD-Pharmingen, San Diego, CA). Primary antibodies were diluted in saponin-containing blocking solution and incubated with the tissue overnight at 4°C followed by repeated washes with PBS. The secondary antibodies were diluted 1:200 and included: goat anti-mouse~Alexafluor 488 (Molecular Probes), donkey anti-rabbit and anti-rat~cy5 (Jackson Immunolabs, West Grove, PN) and donkey anti-rabbit~cy3 (Jackson). In the P7.5 retinas, the EC were visualized with *B. simplicifolia* isolectin coupled to FITC (Sigma) in combination with NG2 or GFAP labeling. For NG2/GFAP colabeling, the NG2 and βgal labeling were completed and the retinas were then incubated with mouse anti-GFAP directly coupled to cy3 (Sigma). The retinas were flat-mounted with anti-fade reagent (Molecular Probes) and observed with an Axiophot upright microscope (LacZ histochemistry) or with a Leica Confocal microscope (immunofluorescence). Image composites were generated by using Adobe Photoshop.

Results

VEGF expression in cocultures of 10T1/2 and EC

To test the hypothesis that mesenchymal cells express VEGF as they differentiate to pericytes, we investigated whether 10T1/2 mesenchymal cells in coculture with EC or treated with TGFβ1, which induces differentiation to pericytes, produce VEGF. VEGFA (hereafter referred to as VEGF) protein in conditioned medium or in cell-associated material was quantified by ELISA. EC cultured alone for up to 96 h expressed negligible amounts of cell-associated (Fig. 1A, top panel) or secreted (Fig. 1A, bottom panel) VEGF. 10T1/2 cells cultured alone for 96 h produced moderate amounts of VEGF, which was distributed equally between CM and cell-associated material. Coculture of 10T1/2 and EC for 96 h led to a greater than twofold increase in total VEGF. In contrast to either cell type alone, the VEGF produced in the cocultures remained largely cell-associated, with less than 10% of VEGF detected in the CM. Results were similar for cocultures grown in serum-free or in 1% serum-containing medium (data not shown).

We have previously shown that 10T1/2 cells cocultured with EC or treated with TGFβ1 differentiate into pericyte-like cells (Darland and D'Amore, 2001; Hirschi et al., 1998). Since the coculture of 10T1/2 and EC increased the expression of VEGF relative to solo cultures, we wanted to determine whether VEGF synthesis was associated with the differentiation of 10T1/2 to pericyte-like cells. Solo cultures of 10T1/2 or EC were cultured in the presence or absence of 3 ng/ml of TGFβ1 or grown in coculture for 3 days, and VEGF levels in cell-associated material and CM were determined (Fig. 1B). EC cultured alone produced negligible levels of detectable VEGF. VEGF levels both in cocultures and in TGFβ1-treated 10T1/2 cells were increased relative to the levels produced by 10T1/2 cells alone. The amount of VEGF in the cocultures was significantly greater than the predicted sum of that produced by the untreated solo cultures (Fig. 1B). The distribution of VEGF between soluble and cell-associated material was approximately equal in the

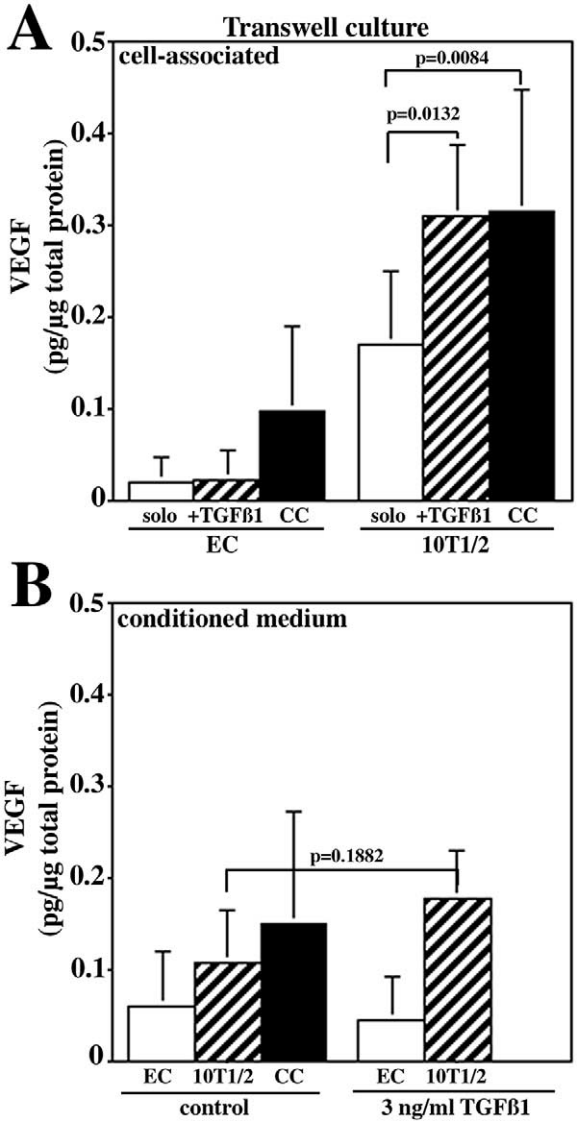

Fig. 2. VEGF expression in solo and cocultures of EC and 10T1/2 cells in Transwell. Solo and cocultures (CC) of 10T1/2 and EC were plated in complete medium at a density of 1.5×10^5 cells/well in Transwell, with the EC plated on the underside of the membrane and the 10T1/2 plated inside the well. After 90 min, the cultures were switched to serum-free medium with or without 3 ng/ml TGFβ1. Cell-associated material (A) and CM (B) were collected at 3 days, and VEGF levels were determined by ELISA. The values shown are the mean and standard deviation of five independent experiments. N.D. is "not detectable."

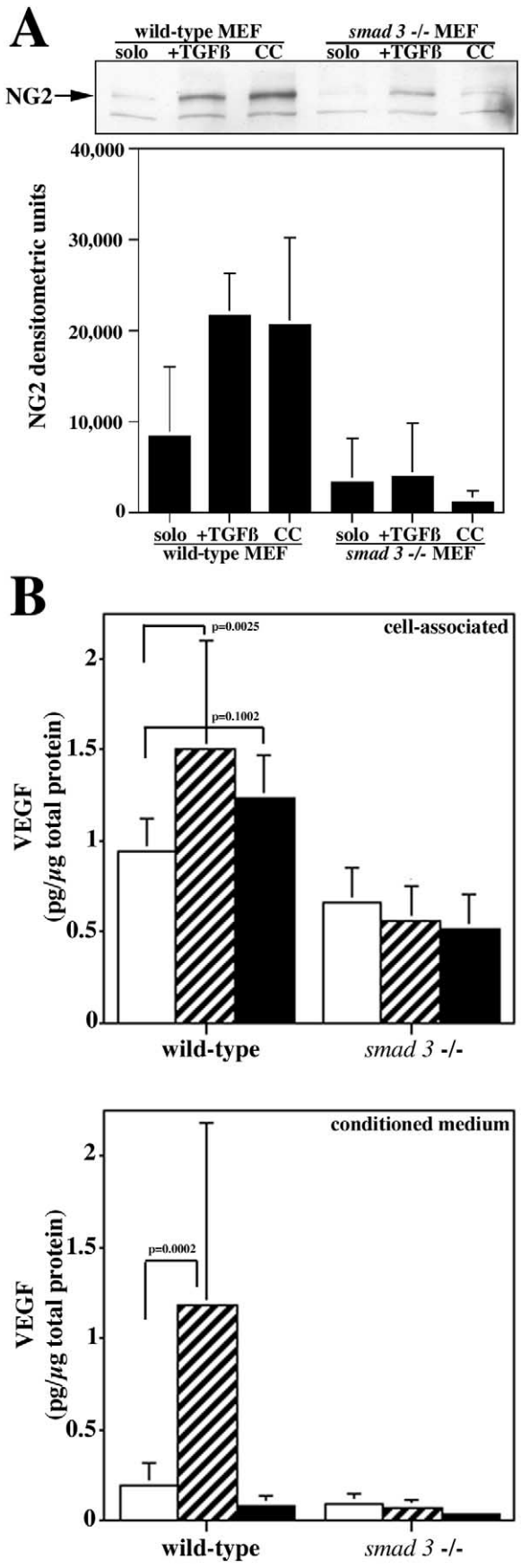

10T1/2 solo cultures both in the presence or absence of TGFβ1. In contrast, coculture of 10T1/2 with EC resulted in marked redistribution of VEGF, with 71% of the total VEGF cell-associated in the coculture (Table 1).

To identify the cell type producing the VEGF in the cocultures, 10T1/2 and EC were cocultured on either side of Transwell membranes or as solo cultures on the Transwell. The porous membrane permits contact between the 10T1/2 and EC while allowing for separation of the two cell types (Saunders and D'Amore, 1992). The solo cultures on the Transwell were also treated with 3 ng/ml of TGFβ1. After 3 days, the cell-associated material and CM were collected and analyzed for VEGF protein (Fig. 2). Once again, the EC cultured alone in Transwell produced low levels of VEGF. 10T1/2 treated with TGFβ1 or grown in coculture with EC produced increased amounts of VEGF compared with the untreated solo 10T1/2 cultures. A low level of VEGF detected in cell-associated material from EC in coculture was likely due to VEGF secreted by 10T1/2 and deposited in the matrix or on the EC surface. The distribution of VEGF between cell-associated and CM was roughly the same (~50% for each) for the solo cultures with or without TGFβ1 treatment (Table 1). However, as for the direct coculture, associated VEGF (74%) in the Transwell cocultures reflected a shift in VEGF localization with heterotypic cell–cell contact. In summary, VEGF is induced in 10T1/2 cells in contact with EC or after treatment with TGFβ, and the majority of the VEGF in the cocultures remains cell-associated.

TGFβ-dependent expression of VEGF

Because there was a consistent increase in VEGF levels in response to TGFβ, we wanted to determine whether TGFβ was mediating the coculture-induced VEGF expression. We have previously found that TGFβ that is activated in cocultures is not fully accessible to exogenously added neutralizing reagents, such as antisera or soluble TGFβ Type II receptor (Darland and D'Amore, 2001). Therefore, to choose an approach to blocking the action of TGFβ1 that would not rely on neutralization, we used mouse embryo

Fig. 3. Effect of smad 3 signal disruption on MEF differentiation and VEGF expression. (A) MEF from wild-type and *smad3*−/− mice were plated at 2.5 × 10^6 cells/well in 6-well tissue culture plates in complete medium. Ninety minutes after plating, the medium was removed and replaced with serum-free medium with or without 3 ng/ml TGFβ1. (A) Cell-associated material was collected after 3 days. Protein concentrations were determined, and 8 μg protein was separated by PAGE and transferred to nitrocellulose. The filters were immunostained for NG2 proteoglycan and band density determined. A representative Western blot for NG2 is shown, and the densitometric values are the mean and standard deviation averaged from three independent experiments. (B) Cell-associated material and CM were collected at 3 days and analyzed for VEGF protein expression by ELISA for solo culture (open bars), solo culture plus 3 ng/ml TGFβ1 (hatched bars), or coculture (CC, closed bars). The values shown are the mean and standard deviation of five independent experiments.

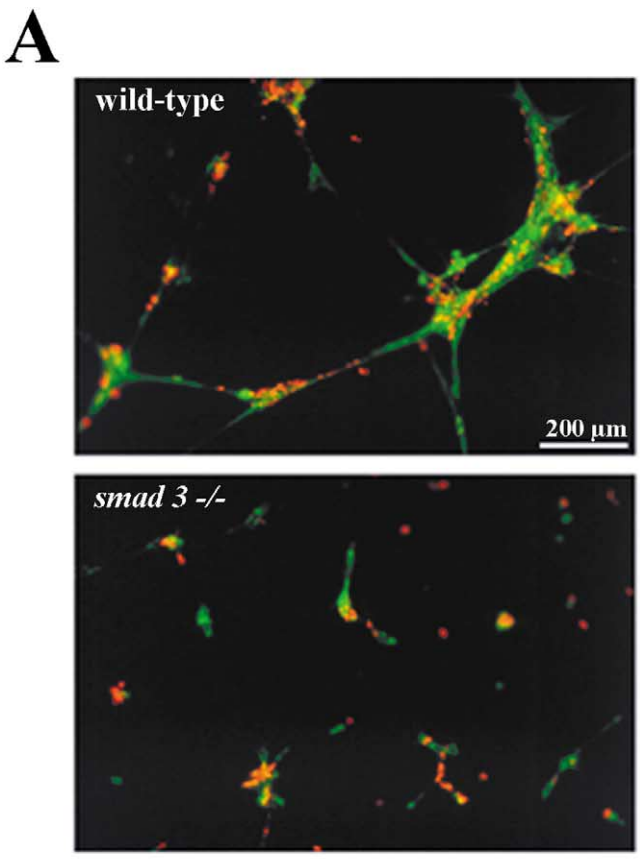

fibroblasts (MEF) derived from *smad3*−/− mice that could not signal through the smad 3 pathway (Piek et al., 2001; Yang et al., 1999). To assess the validity of this approach, we determined whether MEF could respond to TGFβ or coculture with EC by expression of NG2 proteoglycan; a pericyte-associated protein (Grako and Stallcup, 1995; Ozerdem et al., 2001; Schlingemann et al., 1990). The smad 3 null and wild-type MEF were grown alone in the presence or absence of 3 ng/ml of TGFβ1 as well as in direct coculture with EC. Western analysis revealed that coculture or TGFβ treatment of MEF led to increased levels of NG2 proteoglycan (Fig. 3A). In contrast, the smad 3-deficient MEF did not increase NG2 upon coculture with EC and exhibited only a slight increase in NG2 with TGFβ treatment. The increase in NG2 in response to TGFβ in the smad 3 null MEF is likely via the smad 2 pathway.

Since wild-type MEF respond to coculture with EC by differentiating toward a pericyte-like fate, we analyzed VEGF production in the cocultures (Fig. 3B). Wild-type MEF displayed significant baseline VEGF production. Wild-type MEF treated with TGFβ1 or grown in coculture with EC had a small, but significant increase in VEGF production. As was observed for the 10T1/2 cells, VEGF produced by the TGFβ-treated wild-type MEF was equally distributed between cell-associated and CM, whereas a majority of the VEGF in the cocultures remained cell-associated. *Smad3*−/− MEF grown in coculture or treated with TGFβ did not produce increased VEGF.

Since the smad 3 null MEF in coculture with EC were not induced to differentiate to pericytes or to produce VEGF, we wanted to determine whether they could form tube-like structures in a three-dimensional angiogenesis assay as we have previously seen for 10T1/2 (Darland and D'Amore, 2001). When cocultures of EC with either wild-type or smad 3 null MEF were established in Matrigel, EC and wild-type MEF formed cord-like structures, whereas coculture of EC with smad 3-deficient MEF did not form these capillary-like structures and instead formed aggregates (Fig. 4A). Quantification of the structures by measuring cord length (Fig. 4B) revealed distinct differences between the cocultures formed from wild type or smad 3 null fibroblasts. Whereas the wild-type MEF and EC cocultures had structures up to 1500 μm in cord length, the majority of the structures formed in the smad 3 null MEF-EC cocultures were less than 400 μm in length at their longest points. We

Fig. 4. Effect of smad 3 signal disruption on cord formation in 3D cocultures of MEF and EC. Wild-type and *smad 3* null (−/−) MEF were prelabeled with PKH67 (green) and grown in coculture with EC prelabeled with PKH26 (red) at a density of 2.5×10^4 cells/well (24-well plate) on Matrigel. Cord formation in the wild-type fibroblasts cocultured with EC (A, top panel) and the *smad 3* null fibroblasts cocultured with EC (A, lower panel) was visualized at 18 h. Length measurements for the coculture structures were obtained by using NIH Image analysis, and the resulting frequency distribution was graphed for wild-type (B, top panel) and *smad 3* null fibroblasts (B, lower panel). The experiment was repeated three times with similar results, and a representative experiment is shown.

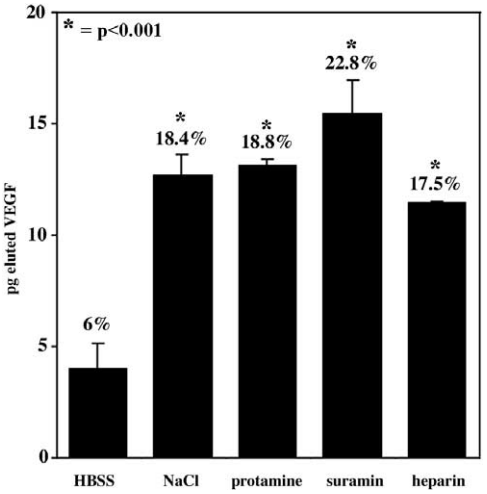

Fig. 5. Determination of cell surface- and matrix-associated VEGF in EC-10T1/2 cocultures. 10T1/2 and EC were plated at 1×10^5 cells/well in 12-well tissue culture plates in complete medium. Ninety minutes after plating, the medium was removed and replaced with serum-free medium. After 3 days, the CM was removed and the wells were washed once with HBSS. Triplicate wells were incubated for 10 min at 37°C with HBSS, 2 M NaCl, 10 mg/ml protamine, 0.2% suramin, or 100 mg/ml heparin. The eluted material and cell-associated material were collected, and VEGF levels were determined by ELISA. The proportion of VEGF eluted is expressed relative to the total VEGF (eluted + cell-associated) for each condition. The experiment was repeated twice with similar results, and a representative experiment is shown.

attempted to rescue cord formation with exogenous application of VEGF164 and VEGF120, but we were unable to induce cord formation in *smad3*−/− MEF-EC cocultures (data not shown).

VEGF localization

Because of the heparan affinity of VEGF164, the predominant coculture isoform (data not shown), we suspected that the VEGF was bound to HSPG on the cell surface and/or the matrix. To test this possibility, 10T1/2 and EC grown in coculture for 3 days were treated with heparin, NaCl, protamine, or suramin, agents all known to release HSPG-bound proteins. The eluted VEGF protein was then measured by ELISA and was expressed relative to the total cell-associated VEGF (Fig. 5). All of the treatments released approximately 20% of the cell-associated VEGF. Repeated sequential incubations or longer incubations did not release significant amounts of additional VEGF (data not shown). Approximately 6% of total VEGF was eluted with the HBSS control. These results indicate that a portion of VEGF produced in cocultures is sequestered on the cell surface or in the matrix.

VEGF-dependent EC survival in coculture

Since the presence of pericytes is associated with vessel stability (Benjamin et al., 1998, 1999) and VEGF supports EC survival, we wanted to determine whether EC survival in cocultures was mediated via a VEGF-dependent mechanism. We therefore examined the effect of VEGF neutralization on cell survival in direct cocultures of 10T1/2 and EC. After 18 h, cocultures of EC and 10T1/2 in the presence or absence of 25 μg/ml VEGF neutralizing antibody were fixed and assessed for apoptotic cells (Fig. 6). The 10T1/2 were distinguished from the EC by immunoreactivity for α-SMA. Neutralization of VEGF led to a 75% increase in EC apoptosis, whereas the 10T1/2 cell apoptosis was unaffected (Fig. 6), indicating that EC survival in coculture is supported by 10T1/2-derived VEGF.

VEGF expression in developing retina

In order to determine the relevance of the in vitro observations to the vasculature in vivo, flat mounts of retinas from mice heterozygous for the LacZ gene under control of the VEGF promoter were examined (Miquerol et al., 1999). Astrocytes have been identified previously as expressing VEGF in the developing retina (Stone et al., 1995, 1996), but little is known about the expression of VEGF in pericytes in vivo. Therefore, we first examined the distribution of NG2-positive pericytes compared with glial fibrillary acidic protein (GFAP)-positive astrocytes at the front of the developing vasculature. Labeling of retinas from postnatal day (P) 7.5 embryos, which have immature retinal vascula-

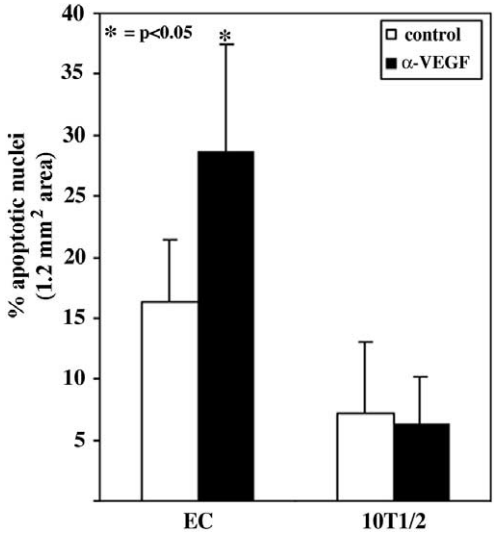

Fig. 6. Role of 10T1/2-derived VEGF on EC apoptosis. EC and 10T1/2 cells were plated in complete medium in 4-well LabTek chamber slides at a total density of 3×10^4 cells/well. After 90 min, the cultures were switched to serum-free medium with 25 μg/ml of neutralizing VEGF antibody (filled bars) or control mouse IgG (open bars). After 18 h, the cells were fixed and stained by DEADEnd assay for apoptotic nuclei. 10T1/2 were distinguished from EC in coculture by immunolabeling with α-SMA, and the cell types were scored separately. The numbers shown are the mean and standard deviation of quadruplicate samples. The experiment was repeated three times with similar results, and a representative experiment is shown.

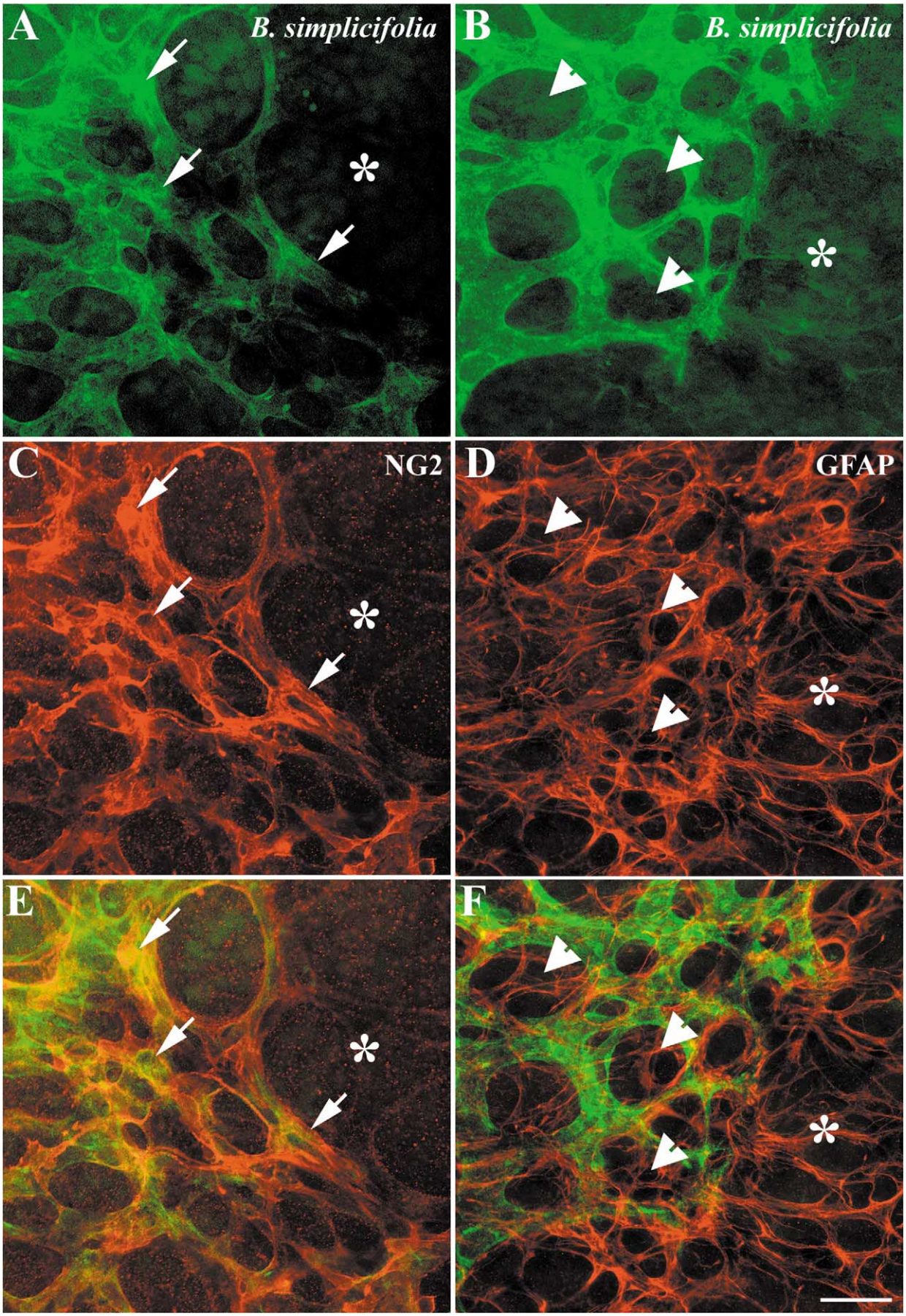
A
B. simplicifolia
B
B. simplicifolia
C
NG2
D
GFAP
E
F

ture and a large avascular zone, with FITC-conjugated *B. simplicifolia* showed new vessel sprouts growing into the avascular periphery (Fig. 7A and B). Parallel retinas stained for either NG2 or GFAP to localize pericytes and astrocytes, respectively (Fig. 7C and D), revealed NG2-positive pericyte processes extending along the newly developing vasculature. An overlay of the images revealed that NG2-positive pericytes (red) are closely associated with the newly forming vessels and, as expected, do not extend into the avascular retina; areas of direct overlap between the EC and pericytes appear yellow (Fig. 7E). In contrast, the overlay of the GFAP (red) and the corresponding lectin showed little overlap (note lack of yellow), though the labeling patterns are similar (Fig. 7F).

We used several approaches to confirm that pericytes in vivo indeed express VEGF. The primary retinal vascular plexus of P 9.5 mice is well established, but is incomplete at the periphery. Histochemical analysis of βgal activity in retinas from P 9.5 mice heterozygous for VEGF-LacZ revealed positive nuclei that were closely associated with microvessel profiles (Fig. 8A). Retinas from P 9.5 mouse neonates were also processed by using the trypsin digest technique, which removes the parenchymal tissue (including neural cells and astrocytes), leaving only the vasculature–endothelial tubes with associated pericytes and smooth muscle cells (Mizutani et al., 1996). We then immunolabeled for βgal (green) and NG2 (blue) to reveal the pericytes that also expressed VEGF-LacZ (Fig. 8B). The NG2-positive pericytes wrap around the vessel tubes, essentially covering the microvascular tree. Trypsin-digested retinas labeled for GFAP revealed that no astrocytes remained associated with the vascular network (data not shown).

Confocal analysis of retinas immunolabeled for NG2 (red), βgal (green), and PECAM (blue) (Fig. 8C) revealed colocalization of βgal-positive nuclei with pericytes in contact with EC, with the most prominent nuclei observed at the vessel branch points. High-power magnification showed the NG2-positive filaments (red) around the βgal-positive nuclei that were most closely associated with the vessels (Fig. 8C, inset). In contrast, βgal-positive nuclei that were located in the intercapillary space were NG2-negative and were presumably astrocytes. To confirm that the cell bodies of the VEGF-producing astrocytes were not directly associated with the capillaries, retinal flat mounts were immunolabeled for the astrocyte marker GFAP (red) in combination with βgal (green) and PECAM (blue) (Fig. 8D). This labeling revealed that the nuclei of the VEGF-producing astrocytes were situated in the intercapillary spaces from where they extended GFAP-positive processes to contact the vasculature (Fig. 8D, inset). Occasional astrocyte nuclei appeared to be located close to a vessel; however, optical sectioning by confocal microscopy revealed that the astrocyte nuclei were, in fact, located in a different plane of focus and had no direct contact with the vessel. The distinct intercapillary localization of astrocyte nuclei was in contrast to the pericyte nuclei that were directly in their characteristic position, apposed to the vessels (Fig. 8A).

To further distinguish between VEGF-expressing pericytes and astrocytes, we labeled retinas with βgal (green), NG2 (blue), and GFAP (red) (Fig. 9). An area of microvasculature was imaged in a series of 10 optical sections representing a z-plane of 5 μm, to confine the compressed image to the vascular surface. NG2 labeling of pericyte processes outlined the vessels in a pattern that is characteristic of pericytes (Fig. 9A) (Sims, 1986). VEGF-expressing cells, indicated by βgal immunoreactivity (Fig. 9B), are dispersed on and between the vasculature. An overlay of NG2 and βgal labeling (Fig. 9C and 9E) reveals that many of the βgal-positive nuclei are surrounded by NG2-positive processes and are localized to capillary branch points, a characteristic feature of pericytes in the retinal vasculature (Kuwabara and Cogan, 1963). Immunolabeling for GFAP revealed astrocyte processes contacting the microvasculature (Fig. 9D and 9F) from somas that were out of the plane of focus.

Discussion

During angiogenesis and vasculogenesis, the microenvironment of a nascent vessel is altered in ways that significantly influence the progression of vessel formation. Local modifiers of vessel formation include growth factors, extracellular matrix, and neighboring cells. Pericytes and EC interact during vessel assembly, and observations of vessel formation in wound healing (Crocker et al., 1970) and in retinal vascularization during development (Benjamin et al., 1998), temporally link vessel stabilization with the presence of pericytes. In the current study, we present data to indicate that interaction of mesenchymal cells (pericyte precursors) with EC leads to the induction of VEGF expression by the pericytes in a TGFβ-dependent event. Further, we provide evidence that pericytes in contact with EC in the developing retinal vasculature in vivo express VEGF.

TGFβ signaling has been implicated as a mediator of heterotypic cell–cell interactions during normal vessel formation in vivo. Mice that lack TGFβ1 (Dickson et al., 1995) or the cognate type II serine/threonine receptor (Oshima et al., 1996) have defective yolk sac hematopoiesis as well as abnormal vasculogenesis. Mice deficient in endoglin, a co-

Fig. 7. Localization of pericytes and astrocytes in developing retina. Retinas from postnatal day 7.5 mice were labeled with *B. simplicifolia* lectin coupled to FITC (green) to localize the developing vasculature. Retinas were then stained for either NG2 to localize pericytes (A, C, E) or GFAP to localize astrocytes (B, D, F). The regions shown are at the periphery of the retina, where the vascular front is extending into the avascular zone (asterisks). The arrows in (A, C, and E) indicate NG2-positive pericytes that are apposed to the capillaries. The arrowheads in (B, D, and F) indicate astrocytes that are widely distributed. The magnification bar is 40 μm.

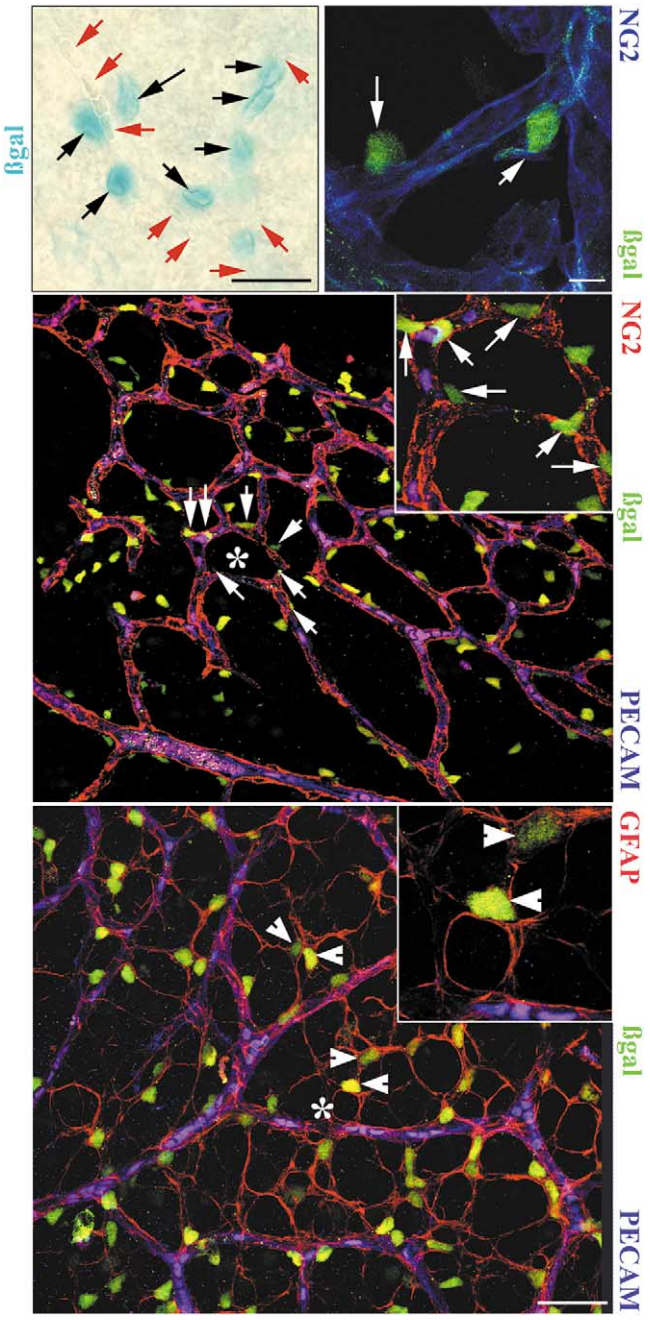

Fig. 8. Localization of VEGF expression in pericytes of the developing retinal vasculature. Retinas from P9.5 VEGF-lacZ +/− mice were analyzed for βgal activity and βgal expression in combination with pericyte- and astrocyte-associated proteins. (A) βgal histochemistry showed positive nuclei (arrows) closely associated with the microvasculature in retinal flat mount (no counterlabeling). Phase bright red blood cells (red arrows) mark the vessel lumen location. (B) Retinas, digested with trypsin to isolate the vasculature free of parenchymal cells, were stained for βgal (green) and NG2 (blue) to reveal pericytes and VEGF expression (arrows). (C) Perivascular nuclei positive for βgal (green) were colocalized with NG2 positive pericytes (red). The asterisk in (C) indicates an area shown in higher magnification (inset) with βgal-positive nuclei associated with NG2-positive pericyte processes (arrows). (D) GFAP-positive astrocytes (red) primarily localized between vessels also expressed βgal (green) (arrowheads). The magnification bars are 40 μm for (A, C, and D), 20 μm for the insets, and 8 μm for (B).

receptor for TGFβ receptors (Barbara et al., 1999), have defective angiogenesis with vessels that are immature and lack normal pericyte and SMC investment (Li et al., 1999). We have previously shown that neutralization of TGFβ in a 3D coculture system blocks cord formation in 10T1/2 and EC cocultures (Darland and D'Amore, 2001). Consistent with these data, we observed that fibroblasts unable to transmit a TGFβ signal via smad 3 (*smad 3*−/−) were unable to form cords in coculture with EC in a 3D angiogenesis assay. While the untreated wild-type MEF have a low basal level of NG2, they are induced to differentiate (express more NG2 protein) and express higher levels of VEGF in response to coculture with EC or after treatment with TGFβ. Therefore, MEF provide a useful system for testing the role of TGFβ in VEGF production. Taken together, our data point to a critical role for TGFβ in regulating pericyte/EC interactions and vessel stabilization; the mechanism of vessel stabilization is not known.

Our evidence suggests that pericyte differentiation is locally regulated and is dependent on heterotypic cell contact. The pericyte-associated proteins, SMA and NG2, are increased in pericyte precursors in response to contact with EC and to TGFβ1 treatment (Darland and D'Amore, 2001; Hirschi et al., 1998). TGFβ is produced by both cell types and is locally activated by a cell contact-dependent mechanism (Antonelli-Orlidge et al., 1989; Sato et al., 1990). Our current findings suggest that 10T1/2 differentiation to pericytes is correlated with VEGF production and sequestration. This correlation may explain the vessel regression that occurs in pericyte-deficient vessels in the developing vasculatures where regression can be prevented by the administration of exogenous VEGF (Benjamin et al., 1998).

Pericyte expression of VEGF in vivo has not been previously examined. Using VEGF-LacZ transgenic mice, we demonstrated VEGF expression by NG2-positive pericytes as well as astrocytes in the developing retinal vasculature. Taken together with our in vitro observations that the pericyte-derived VEGF appears to remain cell-associated, we suggest that contact-induced pericyte differentiation leads to a localized source of VEGF that acts to stabilize newly formed vessels.

The cell-associated localization of VEGF in EC-10T1/2 cocultures differed from that in TGFβ-treated 10T1/2 cells alone where most of the VEGF was detected in the CM. While the switch in localization could be due to changes in VEGF isoform production from the more diffusible VEGF120 to the heparin-binding VEGF164 or 188, RT-PCR analysis of VEGF isoforms in Transwell cocultures did not reveal a significant shift in isoform profile (data not shown). Since a significant proportion of cell-associated VEGF was released via interference with the charge interactions, the cell-associated localization may be mediated, at least in part, by VEGF association with matrix and/or cell surface HSPG.

βgal-positive astrocytes were observed interspersed among the newly formed vasculature. These cells, whose

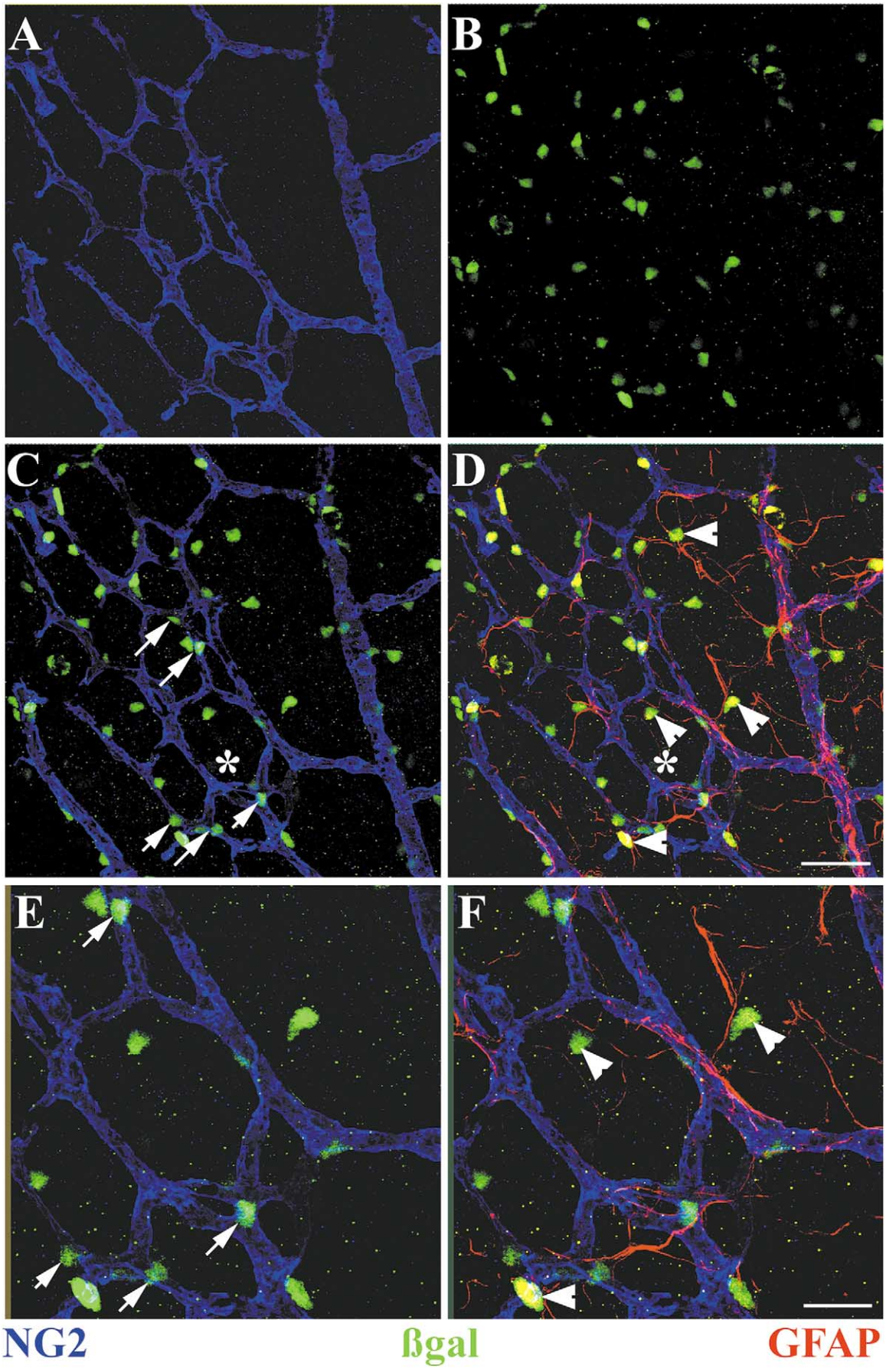
A
B
C
D
E
F
NG2
ßgal
GFAP

nuclei were distinctly located in the intercapillary space, were clearly distinguishable from the pericytes whose nuclei were closely aligned with the vessel wall (Fig. 8). Consistent with previous reports, we observed astrocytes in the avascular zone preceding the vessel front (Stone et al., 1996; Stone et al., 1995) and associated with newly formed vessels (Fig. 7). Though the astrocytes might be considered a source of VEGF for stabilization, the observation of Benjamin et al., in which interference with the association between pericytes and developing vessels (via inhibition of PDGF B) led to vessel regression, indicates that the presence of the astrocytes was insufficient to prevent vessel regression (Benjamin et al., 1998).

It is unlikely that a process as critical as vessel stability would be mediated by a single factor. We suspect that the production of a mature basement membrane (downstream of TGFβ) as part of vessel remodeling also contributes to vessel stabilization, perhaps coming into play at later stages of vessel maturation. Moreover, the angiopoietins clearly participate in vessel stabilization, though the cellular and molecular basis for their actions are not well delineated. Angiopoietin 1, produced by perivascular cells, blocks EC apoptosis in HUVEC cells (Harfouche et al., 2002; Kwak et al., 1999; Papapetropoulos et al., 1999) and stabilizes tumor vasculature in combination with VEGF (Liu et al., 2000; Holash et al., 1999). Recently, application of exogenous angiopoietin 1 has been shown to lead to a partial rescue of the abnormal retinal vessel architecture observed in the absence of mural cells (Uemura et al., 2002); interestingly, however, this effect was predominantly confined to larger vessels. Angiopoietin 2 has been implicated in vessel "destabilization" in several systems, including tumor vessels (Vajkoczy et al., 2002), the pupillary membrane (Lobov et al., 2002), and the heart (Visconti et al., 2002). Thus, it seems clear that vessel stabilization may be governed by a variety of factors, perhaps depending on the tissue and the situation, be it development, maturation or pathology. Regardless of the microenvironment, pericytes are likely to contribute significantly to the integration of the vessel growth and stabilization signals.

Acknowledgments

We thank Dr. William Stallcup (Burnham Institute, La Jolla, CA) and Dr. Anita Roberts (National Cancer Institute, Bethesda, MD) for helpful comments on the manuscript. We thank Dr. Andras Nagy (Samuel Lunenfeld Research Institute, Mt. Sinai Hospital, Toronto, Canada) for the VEGF-LacZ mice and Thanh Truong for help in setting up timed mouse pregnancies. This research was supported by NEI EY05318 (to P.A.D.), Juvenile Diabetes Research Foundation 8352-01 (to P.A.D.), NHLBI10157-02 (to D.D.), and The Knights Templar Eye Foundation (to D.D.). P.A.D. is a Jules and Doris Stein Research to Prevent Blindness Professor.

References

Alon, T., Hemo, I., Itin, A., Pe'er, J., Stone, J., Keshet, S., 1995. Vascular endothelial growth factor acts as a survival factor for newly formed retinal vessels and has implications for retinopathy of prematurity. Nat. Med. 1, 1024–1028.

Antonelli-Orlidge, A., Saunders, K.B., Smith, S.R., D'Amore, P.A., 1989. An activated form of transforming growth factor β is produced by cocultures of endothelial cells and pericytes. Proc. Natl. Acad. Sci. USA 86, 4544–4548.

Barbara, N.P., Wrana, J.L., Letarte, M., 1999. Endoglin is an accessory protein that interacts with the signaling receptor complex of multiple members of the transforming growth factor-β superfamily. J. Biol. Chem. 274, 584–594.

Benjamin, L.E., Golijanin, D., Itin, A., Pode, D., Keshet, E., 1999. Selective ablation of immature blood vessels in tumors follows vascular endothelial growth factor withdrawal. J. Clin. Invest. 103, 159–165.

Benjamin, L.E., Hemo, I., Keshet, E., 1998. A plasticity window for blood vessel remodelling is defined by pericyte coverage of the preformed endothelial network and is regulated by PDGF-B and VEGF. Development 125, 1591–1598.

Carmeliet, P., Ferriera, V., Breier, G., Pollefeyt, S., Kieckens, L., Gertsenstein, M., Fahrig, M., Vandenhoeck, A., Harpal, K., Eberhardt, C., Declercq, C., Pawling, J., Moons, L., Collen, D., Risau, W., Nagy, A., 1996. Abnormal blood vessel development and lethality in embryos lacking a single VEGF allele. Nature 380, 435–439.

Crocker, D.J., Murad, T.M., Greer, J.C., 1970. Role of the pericyte in wound healing. An ultrastructural study. Exp. Mol. Pathol. 13, 51–65.

Darland, D.C., D'Amore, P.A., 2001. TGFβ is required for the formation of capillary-like structures in three-dimensional cocultures of 10T1/2 and endothelial cells. Angiogenesis 4, 11–20.

Denekamp, J., Hobson, B., 1982. Endothelial-cell proliferation in experimental tumors. Br. J. Cancer 46, 711–720.

Dickson, M.C., Martin, J.S., Cousins, F.M., Kulkarni, A.B., Karlsson, S., Akhurst, R.J., 1995. Defective haematopoiesis and vasculogenesis in transforming growth factor-β1 knock-out mice. Development 121, 1845–1854.

Engerman, R.L., Pfaffenbach, D., Davis, M.D., 1967. Cell turnover of capillaries. Lab. Invest. 17, 738–743.

Ferrara, N., Carver-Moore, K., Chen, H., Dowd, M., Lu, L., O'Shea, K., Powell-Braxton, L., Hillan, K.J., Moore, M.W., 1996. Heterozygous embryonic lethality induced by targeted inactivation of the VEGF gene. Nature 380, 439–442.

Fong, G.H., Zhang, L., Bryce, D.M., Peng, J., 1999. Increased hemangioblast commitment, not vascular disorganization, is the primary defect in *flt-1* knock-out mice. Development 126, 3015–3025.

Fig. 9. Distribution of VEGF-producing pericytes and astrocytes in the developing retinal microvasculature. Retinas from P9.5 VEGF-lacZ +/− mice were analyzed for VEGF expression by βgal histochemistry in combination with pericyte- and astrocyte-associated proteins, NG2 and GFAP, respectively. (A) NG2 immunolabeling revealed extensive pericyte processes around the vasculature. (B) βgal immunolabeling revealed VEGF-expressing nuclei throughout the retina. (C) Overlay of the NG2 and βgal immunolabeling revealed that NG2-positive pericytes expressed VEGF (arrows). (D) A third color overlay of GFAP-positive cells revealed the astrocyte processes contacting the vasculature. Asterisks in (C) and (D) indicate areas of higher magnification shown in (E) and (F), respectively. The bars are equal to 40 μm in (A–D) and 20 μm in (E) and (F).

Grako, K.A., Stallcup, W.B., 1995. Participation of the NG2 Proteoglycan in rat aortic smooth muscle cell responses to platelet-derived growth factor. Exp. Cell Res. 221, 231–240.

Harfouche, R., Hasséssian, H.M., Guo, Y., Faivre, V., Srikant, C.B., Yancopoulos, G.D., Hussain, S.N.A., 2002. Mechanisms which mediate the antiapoptotic effects of angiopoietin-1 on endothelial cells. Microvasc. Res. 64, 135–147.

Hellström, M., Gerhardt, H., Kalen, M., Li, X., Eriksson, U., Wolburg, H., Betsholtz, C., 2001. Lack of pericytes leads to endothelial hyperplasia and abnormal vascular morphogenesis. J. Cell Biol. 153, 543–553.

Hellström, M., Kalen, M., Lindahl, P., Abramsson, A., Betsholtz, C., 1999. Role of PDGF-B and PDGFR-β in recruitment of vascular smooth muscle cells and pericytes during embryonic blood vessel formation in the mouse. Development 126, 3047–3055.

Hirschi, K., Rohovsky, S.A., D'Amore, P.A., 1998. PDGF, TGF-β and heterotypic cell-cell interactions mediate the recruitment and differentiation of 10T1/2 cells to a smooth muscle cell fate. J. Cell Biol. 141, 805–814.

Hirschi, K.K., Rohovsky, S.A., Beck, L.H., Smith, S.R., D'Amore, P.A., 1999. Endothelial cells modulate the proliferation of mural cell precursors via platelet- derived growth factor-BB and heterotypic cell contact. Circ. Res. 84, 298–305.

Holash, J., Maisonpierre, P.C., Compton, D., Boland, P., Alexander, C.R., Zagzag, D., Yancopoulos, G.D., Wiegand, S.J., 1999. Vessel cooption, regression, and growth in tumors mediated by angiopoietins and VEGF. Science 284, 1994–1998.

Kuwabara, T., Cogan, D.G., 1963. Retinal vascular patterns. VI. Mural cells of the retinal capillaries. Arch. Ophthalmol. 69, 492–502.

Kwak, H.J., So, J.-N., Lee, S.J., Kim, I., Koh, G.Y., 1999. Angiopoietin-1 is an apoptosis survival factor for endothelial cells. FEBS Lett. 448, 249–253.

Li, D.Y., Sorensen, L.K., Brooke, B.S., Urness, L.D., Davis, E.C., Taylor, D.G., Boak, B.B., Wendel, D.P., 1999. Defective angiogenesis in mice lacking endoglin. Science 284, 1534–1537.

Lindahl, P., Johansson, B.R., Leveen, P., Betsholtz, C., 1997. Pericyte loss and microaneurysm formation in PDGF-B-deficient mice. Science 277, 242–245.

Liu, W., Ahmad, S.A., Reinmuth, N., Shaheen, R.M., Jung, Y.D., Fan, F., Ellis, L.M., 2000. Endothelial cell survival and apoptosis in the tumor vasculature. Apoptosis 5, 323–328.

Lobov, I.B., Brooks, P.C., Lang, R.A., 2002. Angiopoietin-2 displays VEGF-dependent modulation of capillary structure and endothelial cell survival in vivo. Proc. Natl. Acad. Sci. USA 99, 11205–11210.

Miquerol, L., Gertsenstein, M., Harpal, K., Rossant, J., Nagy, A., 1999. Multiple developmental roles of VEGF suggested by a LacZ-tagged allele. Dev. Biol. 212, 307–322.

Mizutani, M., Kern, T., Lorenzi, M., 1996. Accelerated death of retinal microvascular cells in human and experimental diabetic retinopathy. J. Clin. Invest. 97, 2883–2890.

Oshima, M., Oshima, H., Taketo, M.M., 1996. TGF-β receptor type II deficiency results in defects of yolk sac hematopoiesis and vasculogenesis. Dev. Biol. 179, 297–302.

Ozerdem, U., Grako, K.A., Dahlin-Huppe, K., Monosov, E., Stallcup, W.B., 2001. NG2 Proteoglycan is expressed exclusively by mural cells during vascular morphogenesis. Dev. Dyn. 222, 218–227.

Papapetropoulos, A., Garcia-Cardena, G., Dengler, T.J., Maisonpierre, P.C., Yancopoulos, G.D., Sessa, W.C., 1999. Direct actions of angiopoietin-1 on human endothelium: evidence for network stabilization, cell survival, and interaction with other angiogenic growth factors. Lab. Invest. 79, 213–223.

Piek, E., Ju, W.J., Heyer, J., Escalante-Alcalde, D., Stewart, C.L., Weinstein, M., Deng, C., Kucherlapati, R., Bottinger, E.P., Roberts, A.B., 2001. Functional characterization of transforming growth factor β signaling in Smad2- and Smad3-deficient fibroblasts. J. Biol. Chem. 276, 19945–19953.

Sato, Y., Rifkin, D.B., 1989. Inhibition of endothelial cell movement by pericytes and smooth muscle cells: activation of a latent transforming growth factor-beta 1-like molecule by plasmin during co-culture. J. Cell Biol. 109, 309–315.

Sato, Y., Tsuboi, R., Lyons, R., Moses, H., Rifkin, D.B., 1990. Characterization of the activation of latent TGF-β by co-cultures of endothelial cells and pericytes or smooth muscle cells: a self-regulating system. J. Cell Biol. 111, 757–763.

Saunders, K., D'Amore, P.A., 1992. An in vitro model for cell–cell interactions. In Vitro Cell. Dev. Biol. 28A, 521–528.

Schlingemann, R.O., Rietveld, F.J.R., deWall, R.M.W., Ferrone, S., Ruiter, D.J., 1990. Expression of the high molecular weight melanoma-associated antigen by pericytes during angiogenesis in tumors and in healing wounds. Am. J. Pathol. 136, 1393–1405.

Sims, D.E., 1986. The pericyte-a review. Tissue Cell 18, 153–174.

Stone, J., Chan-Ling, T., J., P. e., Itin, A., Gnessin, H., Keshet, E. 1996. Roles of vascular endothelial growth factor and astrocyte degeneration in the genesis of retinopathy of prematurity. Invest. Ophthalmol. Vis. Sci. 37, 290–299.

Stone, J., Itin, A., Alon, T., Pe'er, J., Gnessin, H., Chan-Ling, T., Keshet, E., 1995. Development of retinal vasculature is mediated by hypoxia-induced vascular endothelial growth factor (VEGF) expression by neuroglia. J. Neurosci. 15, 4738–4747.

Uemura, A., Ogawa, M., Hirashima, M., Fujiwara, T., Koyama, S., Takagi, H., Honda, Y., Wiegand, S.J., Yancopoulos, G.D., Nishikawa, S.-H., 2002. Recombinant angiopoietin-1 restores higher-order architecture of growing blood vessels in mice in the absence of mural cells. J. Clin. Invest. 110, 1619–1628.

Vajkoczy, P., Farhadi, M., Gaumann, A., Heidenreich, R., Erber, R., Wunder, A., Tonn, J., Menger, M.D., Breier, G., 2002. Microtumor growth initiates angiogenic sprouting with simultaneous expression of VEGF, VEGF receptor-2, and angiopoietin-2. J. Clin. Invest. 109, 777–785.

Visconti, R.P., Richardson, C.D., Sato, T.N., 2002. Orchestration of angiogenesis and arteriovenous contribution by angiopoietins and vascular endothelial growth factor (VEGF). Proc. Natl. Acad. Sci. USA 99, 8219–8224.

Yang, X., Letterio, J.J., Lechleider, R.J., Chen, L., Hayman, R., Gu, H., Roberts, A.B., Deng, C., 1999. Targeted disruption of SMAD3 results in impaired mucosal immunity and diminished T cell responsiveness to TGF-β. EMBO J. 18, 1280–1291.